Cent. Eur. J. Phys. • 11(2) • 2013 • 213-218
DOI: 10.2478/s11534-012-0152-6

VERSITA

Central European Journal of **Physics**

Characterization of $CaTi_{0.9}Fe_{0.1}O_3/La_{0.98}Mg_{0.02}NbO_4$ composite

Research Article

Aleksandra Mielewczyk-Gryn[1]*, Tomasz Lendze[1], Katarzyna Gdula-Kasica[1], Piotr Jasinski[2], Andrzej Krupa[3], Boguslaw Kusz[1], Maria Gazda[1]

1 *Faculty of Applied Physics and Mathematics, Gdansk University of Technology, Narutowicza 11/12, 80-233 Gdansk, Poland*

2 *Faculty of Electronics, Telecommunication and Informatics, Gdansk University of Technology, Narutowicza 11/12, 80-233 Gdansk, Poland*

3 *The Szewalski Institute of Fluid Flow Machinery, Polish Academy of Science, Fiszera 14, 80-231 Gdansk, Poland*

Received 27 April 2012; accepted 16 October 2012

Abstract: A composite of $CaTi_{0.9}Fe_{0.1}O_3$ and electrolyte material, *i.e.* magnesium doped $La_{0.98}Mg_{0.02}NbO_4$ was prepared and studied. The phase content and the sample microstructure was examined by an X-ray diffraction method and scanning electron microscopy. EDS measurements were done both for composite samples and the diffusion couple. The electrical properties were studied by four terminal DC method. The high-temperature interaction between the two components of the composite has been observed. It has been suggested that lanthanum diffused into the perovskite phase and substituted for calcium whereas calcium and niobium formed the $Ca_2Nb_2O_7$ pyrochlore phase. At 1500°C very large crystallites of the pyrochlore were observed. Regardless of strong interaction between the composite components, its total conductivity was weakly dependent on the sintering temperature.

PACS (2008): 72.80.Tm, 61.05.cp

Keywords: diffusion couple • x-ray diffraction • proton conductors • perovskites

1. Introduction

Proton conducting solid oxide fuel cells (P-SOFCs) can operate at lower temperature than the oxide ion conducting SOFCs [1]. Therefore optimization and development of the composition and microstructure of ceramic materials relevant for P-SOFCs are very important. Electrode materials, because of their complex functions, require further studies. SOFC cathodes should be a good mixed electronic-ionic conductor. It should be permeable for gases (e.g. oxygen or water vapour) and have good catalytic activity for dissociation and reduction of O_2 molecule into oxygen ions. It also should be chemically, structurally and microstructurally stable at high temperatures in the atmosphere of gases present during cell fabrication and work, also, any reaction with the electrolyte,

*E-mail: amielewczyk@mif.pg.gda.pl

which decreases its ionic conductivity, should be avoided. Moreover, the thermal expansion coefficient of a cathode should be as close as possible to those of other parts of a cell. In the case of cathode-supported fuel cells the cathode material should also provide mechanical strength and stability. Also, to create a strong bond between a porous cathode and a dense electrolyte, a similar shrinkage of both materials is required. These requirements often contradict each other and are impossible to be fulfilled simultaneously. For example, high catalytical activity may lead to a material composition change on the surface [2]. High-temperature synthesis and work of the cathode material in contact with the electrolyte facilitates diffusion, reactions and microstructural changes. All of these processes may cause the deterioration of cathodes and cathode supports. On the other hand, a reaction between cathode and electrolyte materials may improve both a bond between them and the mechanical strength of the system.

In the last decade perovskite-type ABO_3 ceramics have had promising applications in SOFCs [3]. Among them, iron-doped calcium titanate $CaTi_{1-x}Fe_xO_3$ (CTF) has been considered as a candidate for a cathode material for proton-conducting SOFCs with lanthanum niobate as an electrolyte [4]. Acceptor-doped lanthanum niobate (LNO) and iron-doped calcium titanate are one of the unconventional electrolyte and cathode materials, respectively, because they have a relatively low conductivity [5]. One of the main advantages of lanthanum niobates is their stability in CO_2 atmosphere. $CaTi_{1-x}Fe_xO_3$ is a mixed ionic-electronic conductor [6] and its thermal expansion coefficient ($\sim 12 \times 10^{-6}$ K^{-1} [7]) is close to that of lanthanum niobate (between 8 and 15×10^{-6} K^{-1} at high and low temperature, respectively [8]). Its electronic conductivity in air is of the p-type, which is considered advantageous from the point of view of a possible cathode material for proton-conducting SOFCs [4]. On the other hand, Fe-doped calcium titanate is a poor proton conductor, with proton transport numbers at 700°C about 0.4% [9]. Therefore, taking advantage of both the $CaTi_{1-x}Fe_xO_3$ and LNO properties requires making a composite material.

In this paper a composite of $CaTi_{0.9}Fe_{0.1}O_3$ (CTF) and electrolyte materials, e.g. magnesium doped $LaNbO_4$ (LMNO) was prepared and studied. Special attention has been paid to the high-temperature interaction between the two components of the composite.

2. Experimental

The $CaTi_{0.9}Fe_{0.1}O_3$ powder was synthesized by the conventional solid state synthesis method described in [10]. The $La_{0.98}Mg_{0.02}NbO_4$ powder was prepared by the molten salt synthesis method (MSS) which was described elsewhere [11]. In order to produce composite samples the powders of CTF and LMNO were mixed in weight ratio 1:1 and then milled in an agate mortar. Then the powders were uniaxially pressed and sintered in the range of temperatures from 1100 to 1500°C for 6 h. To produce diffusion couples the powders were pressed separately and then mounted on one another and sintered at 1200°C for 6 h. The phase composition of the samples were examined by the X-ray diffraction method (XRD) using the Philips X'pert Pro MPD system with the CuKα radiation. The patterns were also analyzed by the Rietveld refinement method using a version of the program LHPM1[1]. The pseudo-Voigt profile function was applied. As a starting point for the analysis crystal structure parameters of $CaTiO_3$ (Space group no. 62, Pbnm) [12] $LaNbO_4$ (space group no. 15, I2/c) [13] and $Ca_2Nb_2O_7$ (Space group no. 227, Fd-3m) [14] were used. The microstructure of samples was investigated by a scanning electron microscope (SEM) Hitachi TM 3000, Zeiss EVO-40 (with Bruker energy dispersive X-ray spectrometer – EDS) and Hitachi S3400N (with Oxford energy dispersive X-ray spectrometer). EDS measurements were done both for composite samples and the diffusion couple. The density of the samples was measured by a classical Archimedes method in kerosene. The porosity was defined as a subtraction between the measured and theoretical density. The electrical properties were studied by the four terminal DC method. The results were corrected for porosity by asymmetric Bruggeman model [15] according to Eq. 1 where σ_0 is the uncorrected conductivity and x is a ratio between the theoretical and measured density. The porosity values in percent are shown in Tab. 1.

Table 1. The porosity values for samples synthesized at various temperatures.

Sintering temperature (°C)	Porosity (%)
1200	36
1300	34
1400	28
1500	12

$$\sigma = \sigma_0(1 - x)^{-3/2} \tag{1}$$

[1] *The X'PERT PLUS Rietveld alghoritm is based on the source codes of the program LHPM1 (April 11, 1988) of R.J. Hill and C.J. Howard, X'Pert Plus, 1999 Philips Electronics N. V.*

3. Results and discussion

The results of the X-ray diffraction analysis are presented in Figs. 1 and 2. Fig. 1 shows XRD patterns of the composite samples sintered at 1100–1500°C. The reflexes characteristic for both lanthanum niobate and calcium titanate are present in all patterns, but it can be seen that the intensity of the reflexes corresponding to the LMNO phase decrease with the increase of sintering temperature. Moreover, even in the case of the sample sintered at 1100°C reflexes of the $Ca_2Nb_2O_7$ pyrochlore may be seen in the spectra. They become larger in the patterns of the samples sintered at higher temperature. In the pattern of the sample sintered at 1500°C reflexes corresponding to the LMNO phase are very low, whereas these the characteristic of the niobium (Nb_2O_5), lanthanum (La_2O_3) and other oxides (magnetite Fe_3O_4 and calcium ferrite $CaFe_4O_5$) can be seen. These results clearly show that there is an interaction between both components of the composite. It leads mainly to the decomposition of the lanthanum niobate phase. In order to analyse quantitative relations between the crystalline phases a Rietveld refinement of the XRD data was performed. An example of the measured plot and the calculated profile obtained for the sample sintered at 1100°C is shown in Fig. 2. The fitted profile R-values are 14, 16, 24 and 30% for the samples sintered at 1100, 1200, 1300 and 1400°C, respectively. Lower quality of the high-temperature results is most probably caused by a preferred orientation of the pyrochlore phase and the possible presence of small amounts of other oxides in the material. The results presented in Tab. 2 showed that the LMNO decomposition is significant above 1300°C. In fact, in the sample sintered at 1300°C approximately 30% of LMNO is decomposed. On the other hand the changes undergone by calcium titanate in the sintering process are apparently more subtle. It does not decompose, but it should be noted that calcium originating from CTF, together with niobium from LMNO, forms the pyrochlore phase. Rietveld analysis shows a gradual increase of the volume of the crystal unit cell with the increase of the sintering temperature. So that, we suggest that the main process in which CTF takes part is a substitution of calcium by lanthanum. V. Vashook *et al.* found that the substitution of calcium by lanthanum in calcium titanate $Ca_{1-x}La_xTiO_3$ for x up to 0.3 occurs without a structural distortion and it is accompanied by a unit cell expansion of about 2.4% [16]. Similar increase of the CTF unit cell volume (1.9%) was observed in the case of the sample annealed at 1500°C. This hypothesis is further supported by the observation that only low reflexes corresponding to lanthanum oxide are detected by XRD in the samples. The expansion of unit cell of CTF may be

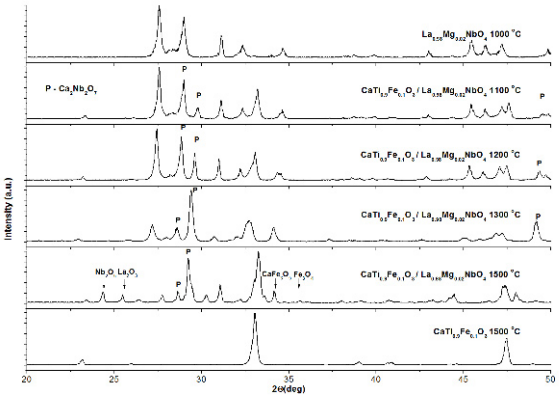

Figure 1. X-ray diffraction patterns of LMNO and CTF initial powders and the composite samples sintered at 1100–1500°C.

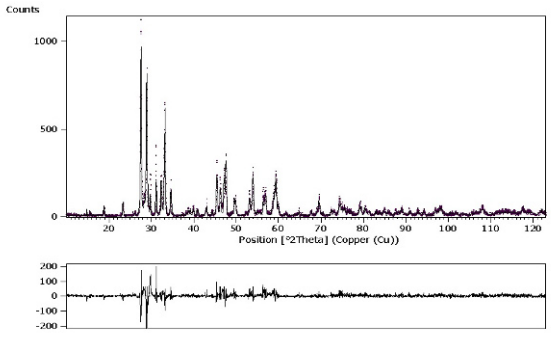

Figure 2. Observed (solid line) and calculated (dotted line) diffraction patterns for LMNO/CTF composite sample sintered at 1100°C. The lower curve shows the difference between observed and calculated patterns.

also caused by a process of dissolving of the pyrochlore in the CTF which is linked with unit cell expansion as well [17].

In Fig. 3 a and b the SEM micrographs of the surface of the LMNO-CTF composite sample sintered at 1400°C are presented. The difference between two components of the composite is clearly visible. EDS measurements of grains showed that bright agglomerates noticeable in Fig. 3b are composed of the LMNO phase while the darker grains are the CTF phase. The LMNO agglomerates are quite large; their size reaches approximately 10 μm. This fact is in agreement with previous studies of sintered LMNO samples published elsewhere which proved that in the case of sintered samples prepared from MSS powders grains tend to agglomerate [11]. On the other hand the CTF grains are not so strongly agglomerated and have average sizes of 3–5 μm. Fig. 4 depicts the SEM micrograph of the surface of

Table 2. The crystal unit cell parameters and phase content values achieved by Rietveld analysis for samples synthesizedn at different temperatures.

Sintering temperature	1100 ℃	1200 ℃	1300 ℃	1400 ℃
CTF				
Crystal structure	tetragonal space group Pnma (62)			
a (Å)	5.4436(4)	5.4597(6)	5.415(2)	5.466(1)
b (Å)	7.6507(6)	7.6483(8)	7.684(1)	7.706(2)
c (Å)	5.3917(4)	5.3904(9)	5.464(1)	5.4341(7)
V ($Å^3$)	224.55	225.09	226.28	228.84
Content (%)	47	41	50	50
LMNO				
Crystal structure	monoclinic space group C 2/c (15)			
a (Å)	7.3516(3)	7.3483(9)	7.355(1)	7.427(3)
b (Å)	11.5318(5)	11.8262(6)	11.535(2)	11.542(8)
c (Å)	5.2078(2)	5.2068(8)	5.213(1)	5.303(3)
β (^{o})	130.970(3)	130.973(3)	131.1	131.79(3)
V ($Å^3$)	332.32	332.45	332.7	333.5
Content (%)	49	46	32	18
Pyrochlore				
Crystal structure	regular space group Fd-3m (277)			
a (Å)	10.4263(8)	10.4372(5)	10.4330(5)	10.359(3)
V ($Å^3$)	1133.433	1136.97	1132.605	1111.615
Content (%)	4	13	18	32

the sample sintered at 1500℃. The sample morphology is very different from the one sintered at lower temperature. The sample surface is covered with very large plate-like grains. Their size (up to 30 μm) is much larger than the size of crystallites formed at lower temperature. Forming such large crystals was previously observed both in perovskite [18] and pyrochlore [19] groups of compounds. It should be noted that neither in the single-phase lanthanum niobate nor iron-doped calcium titanate sintered at 1500℃ such a phenomenon occured. The XRD results indicate that the large crystals are $Ca_2Nb_2O_7$ pyrochlore. The melting temperature of a single phase $Ca_2Nb_2O_7$ is 1571℃ [20]. On the other hand, Roth *et al.* while describing the phase relations between $CaTiO_3$ and $Ca_2Nb_2O_7$ showed that solidus temperature in this binary system is between 1470 and 1550℃ [17]. So that, at 1500℃ liquid phase may form in the material and, as a result, the rate of crystal growth of the pyrochlore may be relatively high.

In order to investigate in details the reaction between calcium titanate and lanthanum niobate the diffusion couples of the two phases were prepared and the EDS measurements were carried out. Fig. 4 shows the EDS analysis results of the diffusion couple sintered at 1200℃. The scan was taken along the line perpendicular to the interface between CTF and LMNO phase (marked by a dashed line in Fig. 5a). The results show that the initial interface between the LMNO and the CTF phases shifted during the sintering process. The diffusion of lanthanum and niobium atoms into the CTF side can be observed. It confirms the XRD results showing that it is lanthanum niobate which decomposes as a result of the interaction with calcium titanate. What is very interesting, the iron content first increases, reaches a small maximum and then decreases again while the calcium and titanium content decreases monotonically. The iron content rise is only visible at the interface between the samples where the interaction between both phases occurs. This phenomenon may be associated with the interaction between the phases of the composite observed by XRD. As a result of the substitution of calcium by lanthanum in calcium titanate and formation of the pyrochlore a considerable number of iron atoms originating from the CTF may form iron oxides. Indeed, the presence of magnetite and calcium ferrite was detected in the samples sintered at 1500℃, for which the decomposition of the initial compounds is the most visible.

Fig. 6 presents the Arrhenius plot of total conductivity in atmospheric air of the LMNO/CTF composite samples corrected for the porosity. It is apparent that the conductivity level in the case of samples sintered at 1500℃ is higher than for the other samples and reaches value of 5×10^{-4} S cm^{-1} at 600℃. In the case of lower sintering temperature this value is lower approximately

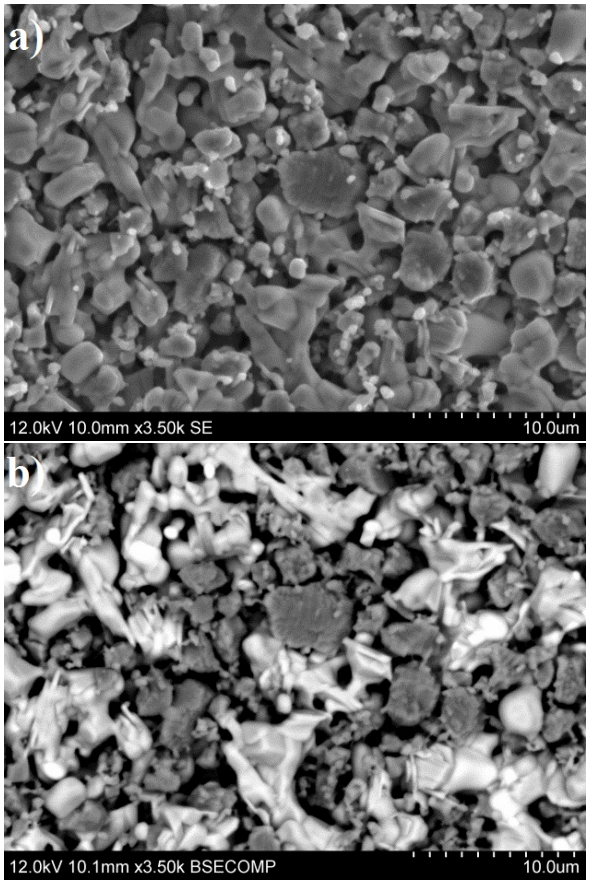

Figure 3. SEM micrographs of the sample sintered at 1400°C taken by a) secondary electron, b) backscatter electron detector.

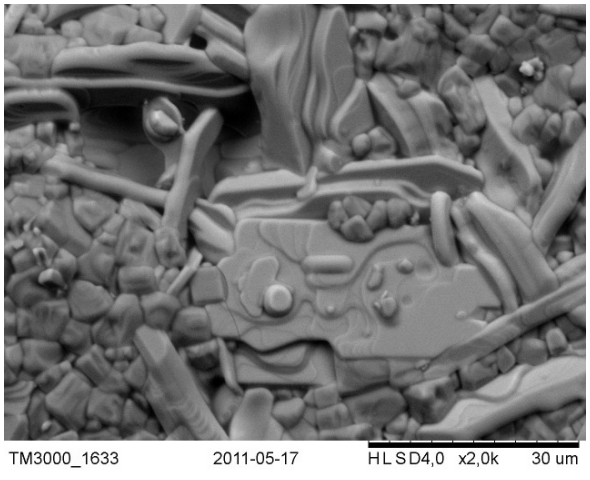

Figure 4. SEM micrograph of the sample synthesized at 1500°C.

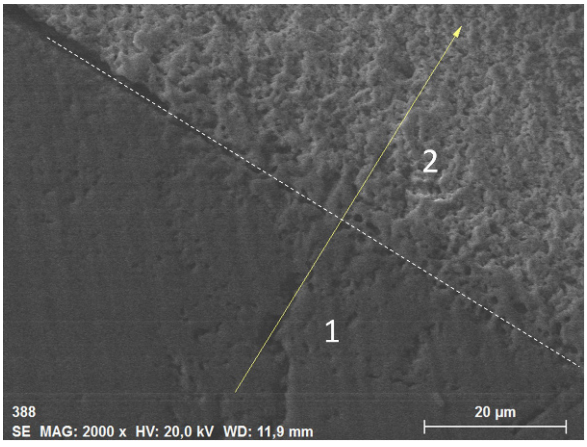

(a)

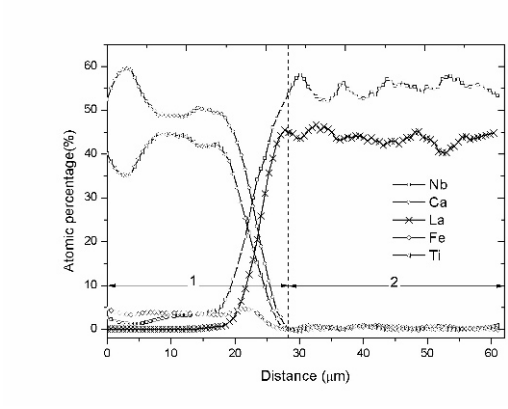

(b)

Figure 5. (a) Secondary electron micrograph of the LMNO/CTF diffusion couple following 12 h firing at 1200°C in air. (b) Phase composition taken along the marked line in (a). The numbered regions match to those marked in (a).

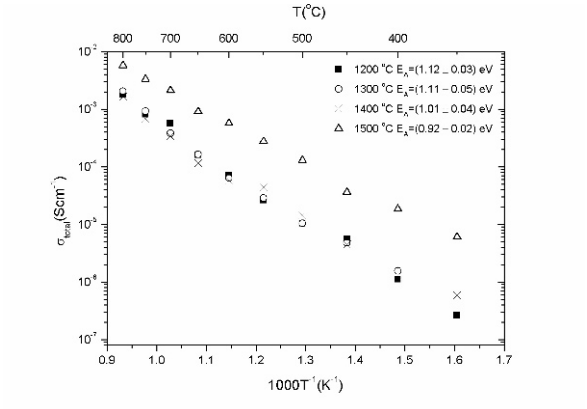

Figure 6. Temperature dependence of total conductivity in atmospheric air of the LMNO/CTF composite samples sintered at different temperatures. The conductivity data have been corrected for the porosity.

6×10^{-5} S cm^{-1}. It means that regardless strong interaction between the composite components its total conductivity rather weakly depends on the sintering temperature. Relatively high conductivity of the sample sintered at 1500°C can be explained by the formation of the conducting secondary phases. For instance the presence of the magnetite phase (Fe_3O_4) may increase the total conductivity of the composite since its conductivity (10^2 S cm^{-1} at 585°C) is considerably higher than that of both CTF and LMNO [21, 22]. The other secondary phase $CaFe_2O_5$ has been also reported as electronic conductor [23]. The apparent activation energy values for all samples are similar but they are slightly decreasing with the rise of sintering temperature from 1.12 eV for 1200°C to 0.92 eV for 1500°C. The values of apparent activation energy are both higher than in case of pure LMNO (approximately 0.7 eV [24]) and CTF (approximately 0.5 eV [10]). This indicates that the process of conduction for composite samples is different than in the case of pure compounds, which is related to the presence of the secondary phases in the composite apart from LMNO and CTF.

4. Conclusions

A composite of $CaTi_{0.9}Fe_{0.1}O_3$ (CTF) and electrolyte materials, that is, magnesium doped $La_{0.98}Mg_{0.02}NbO_4$ (LMNO) was prepared and studied. The high-temperature interaction between the two components of the composite has been observed. The diffusion of lanthanum and niobium from the LMNO phase towards CTF has been observed. It has been suggested that lanthanum diffused into the perovskite phase and substituted for calcium whereas calcium and niobium formed the $Ca_2Nb_2O_7$ pyrochlore phase. The larger sintering temperature, the larger amount of LMNO decomposed. Microstructure of the composite depended on the sintering temperature. In the samples sintered below 1500°C the microstructure was typical of ceramic-ceramic composite. At 1500°C very large crystallites of the pyrochlore were observed. Regardless of strong interaction between the composite components its total conductivity was weakly dependent on the sintering temperature. Summing up, despite very interesting properties of doped calcium titanate it seems it is not suitable as a cathode material in the SOFC with lanthanum niobate as an electrolyte.

References

[1] L. Cindrella et al., J. Power Sources 194, 146 (2009)
[2] J.E. Elshof, H.J.M. Bouwmeester, H. Verweij, Appl. Catal. A-Gen. 30, 195 (1995)
[3] S.M. Haile, Acta Mater. 51, 5981 (2003)
[4] A. Magraso et al., Fuel Cells 11, 17 (2011)
[5] F.M. Figueiredo, V.V. Kharton, J.C. Waerenborgh, A.P. Viskup, E.N. Naumovich, J.R. Frade, J. Am. Ceram. Soc. 87, 2252 (2004)
[6] L.A. Donyushkina, A.K. Demin, B.V. Zhuravlev, Solid State Ionics 116, 85 (1999)
[7] F.M. Figueiredo, V.V. Kharton, A.P. Viskup, J.R. Frade, J. Membrane Sci. 236, 73 (2004)
[8] T. Mokkelbost, H.L. Lein, P.E. Vullum, R. Holmestad, T. Grande, M.-A. Einarsrud, Ceram. Int. 35, 2877 (2009)
[9] L.A. Dunyushkina, A.V. Kuzmin, V.B. Balakireva, V.P. Gorelov, Russ. J. Electrochem+. 42, 375 (2006)
[10] T. Lendze A. Mielewczyk-Gryn, K. Gdula, B. Kusz, M. Gazda, Advances in Materials Sciences 1, 55 (2011)
[11] A. Mielewczyk-Gryn, K. Gdula, T. Lendze, B. Kusz, M. Gazda, Cryst. Res. Technol. 12, 1225 (2010)
[12] X. Liu, R.C. Liebermann, Phys. Chem. Miner. 20, 171 (1993)
[13] S. Tsunekawa, T. Kamiyama, K. Sasaki, H. Asano, T. Fakuda, Acta Crystallogr. A 49, 595 (1993)
[14] J.T. Lewandowski, I.J. Pickering, Mater. Res. Bull. 27, 981 (1992)
[15] D.A.G. Bruggeman, Ann. Phys.-Berlin 416, 636 (1935)
[16] V. Vashook, L. Vasylechko, M. Knapp, H. Ullmann, U. Guth, J. Alloy. Compd. 354, 13 (2003)
[17] R.S. Roth et al., J. Solid State Chem. 181, 406 (2008)
[18] M. Baurer, S.-J. Shih, C. Bishop, M.P. Harmer, D. Cockayne, M.J. Hoffmann, Acta Mater. 58, 290 (2010)
[19] S.H. Yoon, Y.-S. Park, J.-Oh Hong, D.-S. Sinn, J. Mater. Res. 22, 2539 (2007)
[20] S.C. Hopkins, Ph.D. thesis, Sidney Sussex College, (Cambridge, United Kingdom, 2007)
[21] P.A. Miles, W.B. Westphal, V.A. Hippel, Rev. Mod. Phys. 29, 279 (1957)
[22] A. Fursina, Ph.D. thesis, Rice University, (Texas, USA, 2010)
[23] C. Gleitzer, J.B. Goodenough, Struct. Bond. 6, 1 (1985)
[24] A. Mielewczyk-Gryn, K. Gdula, S. Molin, P. Jasinski, B. Kusz, M. Gazda, J. Non-Cryst. Solids 356, 1976 (2010)